Molecular Systems Biology 6; Article number 447; doi:10.1038/msb.2010.103
Citation: ***Molecular Systems Biology* 6:447**

www.molecularsystemsbiology.com

molecular systems biology

Emergence of tissue polarization from synergy of intracellular and extracellular auxin signaling

Krzysztof Wabnik[1,2,3,6], Jürgen Kleine-Vehn[1,2,6,*], Jozef Balla[4], Michael Sauer[1,2,7], Satoshi Naramoto[1,2], Vilém Reinöhl[4], Roeland MH Merks[1,2,8], Willy Govaerts[3] and Jiří Friml[1,2,5,*]

[1] Department of Plant Systems Biology, VIB, Ghent University, Gent, Belgium, [2] Department of Plant Biotechnology and Genetics, Ghent University, Gent, Belgium, [3] Department of Applied Mathematics and Computer Science, Ghent University, Gent, Belgium, [4] Department of Plant Biology, Mendel University, Brno, Czech Republic and [5] Department of Experimental Biology, Masaryk University, Brno, Czech Republic
[6] These authors contributed equally to this work
[7] Present address: Departamento de Genética Molecular de Plantas, Centro Nacional de Biotecnología, Consejo Superior de Investigaciones Científicas, Madrid 28049, Spain
[8] Present address: Centrum Wiskunde & Informatica, 1098 XG Amsterdam, and Netherlands Consortium for Systems Biology, 1098 XG Amsterdam, The Netherlands
* Corresponding authors. J Friml or J Kleine-Vehn, Department of Plant Systems Biology, VIB, Ghent University, Technologiepark 927, B-9052 Gent, Belgium.
Tel.: + 32 9 3313913; Fax: + 32 9 3313809; E-mail: jiri.friml@psb.vib-ugent.be or Tel.: + 32 9 3313946; Fax: + 32 9 3313809; E-mail: jurgen.kleine-vehn@psb.vib-ugent.be

Received 25.5.10; accepted 2.11.10

Plant development is exceptionally flexible as manifested by its potential for organogenesis and regeneration, which are processes involving rearrangements of tissue polarities. Fundamental questions concern how individual cells can polarize in a coordinated manner to integrate into the multicellular context. In canalization models, the signaling molecule auxin acts as a polarizing cue, and feedback on the intercellular auxin flow is key for synchronized polarity rearrangements. We provide a novel mechanistic framework for canalization, based on up-to-date experimental data and minimal, biologically plausible assumptions. Our model combines the intracellular auxin signaling for expression of PINFORMED (PIN) auxin transporters and the theoretical postulation of extracellular auxin signaling for modulation of PIN subcellular dynamics. Computer simulations faithfully and robustly recapitulated the experimentally observed patterns of tissue polarity and asymmetric auxin distribution during formation and regeneration of vascular systems and during the competitive regulation of shoot branching by apical dominance. Additionally, our model generated new predictions that could be experimentally validated, highlighting a mechanistically conceivable explanation for the PIN polarization and canalization of the auxin flow in plants.
Molecular Systems Biology **6**: 447; published online 21 December 2010; doi:10.1038/msb.2010.103
Subject Categories: simulation and data analysis; plant biology
Keywords: auxin; canalization; cell polarity; PIN proteins

Introduction

A key question in developmental biology relates to the fundamental issue of how an individual cell in a polarized tissue senses the polarities of its neighbors and its position within the tissue. In plant development, this issue is of pronounced importance, because plants have the remarkable ability to redefine cell and tissue polarities in different developmental programs, such as embryogenesis, postembryonic organogenesis, vascular tissue formation, and tissue regeneration (Kleine-Vehn and Friml, 2008).

In 1880, Charles Darwin predicted that a growth-stimulating molecule directionally moves within plant tissues (Darwin and Darwin, 1880). This growth regulator was later on termed auxin and represents the first isolated phytohormone. Intercellular auxin transport, in conjunction with local auxin biosynthesis, is postulated to define auxin gradients during embryonic and postembryonic development, giving positional cues for primordium formation, organ patterning, and tropistic growth (Friml *et al*, 2002; Benková *et al*, 2003; Reinhardt *et al*, 2003; Heisler *et al*, 2005; Scarpella *et al*, 2006; Dubrovsky *et al*, 2008). The direction of the auxin transport depends largely on the polar subcellular localization of PINFORMED (PIN) proteins at the plasma membrane (Petrášek *et al*, 2006; Wiśniewska *et al*, 2006). As the molecular basis of the PIN polarization in plants remains unexplored, theoretical and experimental insights into mechanisms that regulate the PIN polarity are of outstanding interest to plant biologists.

PIN proteins recycle between the plasma membrane and the intracellular endosomal compartments (Geldner *et al*, 2001; Dhonukshe *et al*, 2007). This recycling modulates PIN-dependent auxin efflux rates and enables rapid changes in

PIN polarity (Dhonukshe *et al*, 2008; Kleine-Vehn *et al*, 2008a). Additionally, auxin interferes with the PIN recycling by inhibiting the PIN protein internalization (Paciorek *et al*, 2005).

At the tissue level, polarization of PIN proteins in individual cells has been suggested to be coordinated in the surrounding cells by a positive feedback between auxin and its directional transport (Mitchison, 1980; Sauer *et al*, 2006). As the molecular mechanism for PIN polarization still needs to be unraveled, numerous theoretical studies have been applied to test various hypotheses. In the canalization hypothesis (Sachs, 1981), an underlying positive feedback loop exists between the auxin-flux and auxin-transport capacity of cells, ultimately canalizing auxin progressively into discrete channels. It incorporates a hypothetical flux sensor component as an essential part of the auxin feedback mechanism for PIN polarization (Mitchison, 1980) and is widely exploited in so-called flux-based models to study PIN-dependent developmental processes, such as venation patterning in leaves (Rolland-Lagan and Prusinkiewicz, 2005; Sauer *et al*, 2006; Scarpella *et al*, 2006). On the basis of the experimental observation of adverse PIN polarization during phyllotactic patterning in vegetative shoot apical meristems (Reinhardt *et al*, 2003), PIN proteins have been proposed to orient to the side of the cell that faces the neighboring cell with the highest auxin concentration (Jönsson *et al*, 2006; Smith *et al*, 2006). This alternative hypothesis integrates an unknown short-range intercellular signal, transmitting the auxin concentration of its direct neighbors (Sahlin *et al*, 2009). Concentration-based models can reproduce various phyllotactic patterns occurring in planta (Reinhardt *et al*, 2003; Jönsson *et al*, 2006; Smith *et al*, 2006) and initiation of the primary leaf vein (Merks *et al*, 2007).

The flux-based (Mitchison, 1980; Rolland-Lagan and Prusinkiewicz, 2005) and concentration-based models (Merks *et al*, 2007) provide conceptually different frameworks for PIN polarization during venation patterning in plants. Unless additional assumptions are included (Feugier *et al*, 2005), these models predict the low auxin concentration in vein precursors, which contradicts the experimental observations of high auxin signaling in developing veins (Scarpella *et al*, 2006).

To assess this issue, flux-based and concentration-based models were combined into a dual polarization model, in which the dominating mechanism depends on the actual auxin content of the cells (Bayer *et al*, 2009). This model generates the simultaneous appearance of high auxin concentration in emerging veins and recapitulates PIN polarization and auxin transport during early midvein formation and phyllotaxis.

Nevertheless, biological evidence for a hypothetical flux sensor (Mitchison, 1980; Rolland-Lagan and Prusinkiewicz, 2005; Bayer *et al*, 2009) and/or a short-range signal (Jönsson *et al*, 2006; Smith *et al*, 2006; Merks *et al*, 2007; Bayer *et al*, 2009) for PIN polarization remains difficult to identify. To overcome this problem, individual cells have been suggested to read out hypothetical intracellular auxin gradients to polarize PIN proteins by a yet to be clarified perception mechanism (Kramer, 2009). Based solely on the steepness of this internal auxin gradient (independently of the overall auxin concentrations), PIN proteins would polarize toward the side of the cell with the lowest intracellular auxin concentration (Kramer, 2009). This model predicts that a conductive auxin channel originates from an auxin sink instead of an auxin source, whereas experimental observations suggest the opposite (Sauer *et al*, 2006).

Here, we propose a novel, biologically plausible model for PIN polarization that combines intracellular and extracellular auxin signaling as a unifying approach for tissue polarization in plants. The model integrates experimental data, such as auxin feedback on PIN transcription (Peer *et al*, 2004; Heisler *et al*, 2005) via a nuclear auxin signaling pathway (Chapman and Estelle, 2009) and auxin feedback on PIN endocytosis (Paciorek *et al*, 2005) via the hypothetical, yet conceivable assumption of extracellular auxin perception. The extracellular receptor-based polarization (ERP) model faithfully reproduces PIN polarization and auxin distribution patterns during vascularization, tissue regeneration, vein connection, generation of leaf vein loops, and competitive auxin canalization for axillary bud outgrowth. The detailed analysis of our model revealed new mechanistic insights into initiation, maintenance, and robustness of PIN polarization during venation patterning and tissue regeneration. Remarkably, the ERP model generated new predictions that were experimentally validated. The versatility and accuracy of model predictions highlight the importance and plausibility of dual auxin perception for PIN polarization and auxin-driven plant development.

Results

Assumptions of the ERP model

Tissue polarization requires cell-to-cell communication, but, in plants, a biologically conceivable mechanism for PIN polarization was elusive. Therefore, we assumed that the extracellular space (apoplast) provides a relatively easy mean for a direct and simple cell-to-cell communication by the competitive utilization of one or more signaling components (receptors). Notably, the first isolated auxin-binding protein (ABP1) has been proposed to be secreted and to be active in the apoplast (for review see Napier *et al*, 2002; Tromas *et al*, 2009), indicating the possibility for extracellular auxin signaling.

Auxin exerts its action to a large extent by modulating gene expression via binding to the well-characterized nuclear auxin receptor TIR1 (reviewed in Chapman and Estelle, 2009). Here, we explored the simplest, yet biologically plausible, scenario in which auxin would act both intracellularly on PIN expression and extracellularly on the subcellular dynamics of PIN proteins via receptor-mediated signaling pathways.

The computational approach to model the PIN polarization integrated available molecular and cell biological data. Biological data (I) and hypothetical assumptions (II) were incorporated into a computer model for auxin transport and PIN polarization (for model details see Supplementary information and Supplementary Tables 1–3).

(I) The auxin fluxes were modeled between discrete cells and cell wall compartments by using the chemiosmotic hypothesis (Goldsmith *et al*, 1981; Figure 1A). Accordingly, auxin slowly diffused and was actively transported by the

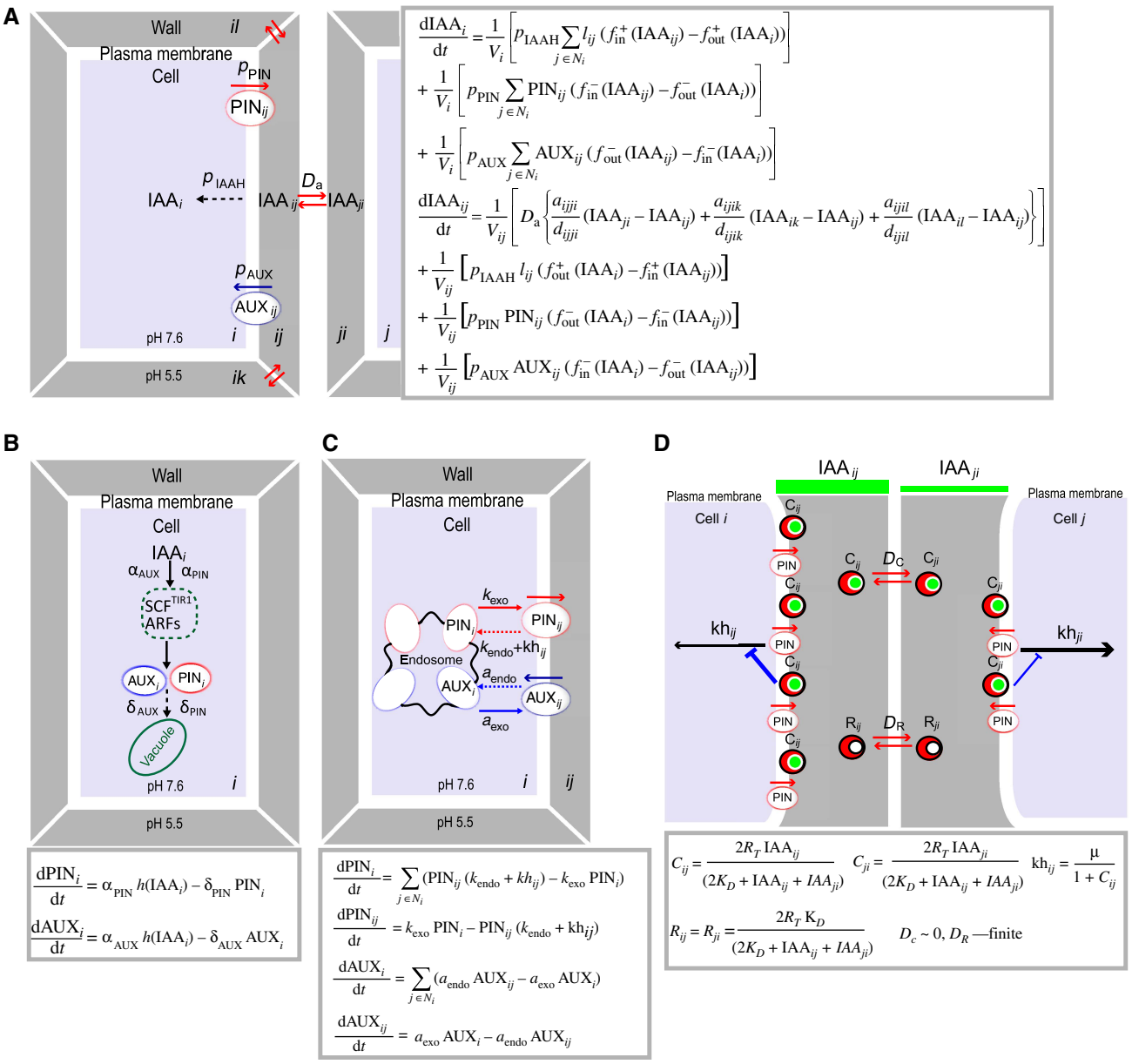

Figure 1 Schematic and mathematical representations of the main model assumptions. (**A**) Schematic and mathematical representations of auxin transport between cells (*i*, *j*) and cell wall interfaces (*ij*, *ji*, *ik*, and *il*). IAA_i describes the mean auxin concentration in the *i*th cell; whereas IAA_{ij} and IAA_{ji} determine the auxin concentrations in discrete wall compartments (*ij* and *ji*). The functions f_{in}^{+}/f_{in}^{-} and f_{out}^{+}/f_{out}^{-} are used to evaluate the fractions of auxin in the cell and in the cell wall. Dashed arrows indicate the rate of passive auxin diffusion into the cell and p_{IAAH} describes the membrane permeablility for protonated auxin. D_a is the diffusion coefficient of auxin between neighboring wall compartments. p_{PIN} and p_{AUX} are parameters that determine PIN- and AUX/LAX-dependent efflux and influx of auxin across the plasma membrane, respectively. PIN_{ij}/PIN_{ji} and AUX_{ij}/AUX_{ji} are PIN (red) and AUX/LAX (blue) levels, respectively, in neighboring plasma membranes. (**B**) Schematic and mathematical representations of intracellular auxin perception: auxin-induced carrier synthesis (solid black arrows) and basic carrier degradation (dashed black arrows). The α_{PIN} and α_{AUX} are the rates of auxin-dependent *PIN* and *AUX/LAX* expression, respectively. The degradation rates of PIN and AUX/LAX proteins are given by parameters δ_{PIN} and δ_{AUX}. (**C**) Schematic and mathematical representations of auxin carrier trafficking. The rates of endo- and exocytosis affect carrier abundance at the plasma membrane. PIN_i corresponds to the PIN level at the plasma membrane of the *i*th cell (red arrows) and AUX_i determines the AUX/LAX level (blue arrows) in the *i*th cells. The base rates for PIN exocytosis and PIN endocytosis are k_{exo} and k_{endo}, whereas a_{exo} and a_{endo} similarly correspond to AUX/LAX recycling rates. The component kh_{ij} determines the inhibitory effect of auxin on the PIN internalization at a given cell side. (**D**) Schematic and mathematical representations of extracellular receptor-based auxin signaling pathway for modulation of PIN trafficking. Two adjacent cells share a common pool of extracellular auxin receptors denoted as $2R_T = C_{ij} + C_{ji} + R_{ij} + R_{ji}$, where C_{ij} and C_{ji} represent the levels of the auxin-bound receptor in the discrete wall compartments facing the surfaces of the adjacent cells *i* and *j*. R_{ij} and R_{ji} correspond to the levels of free receptors that undergo diffusion between common wall compartments (D_R). The auxin receptors are activated by auxin via direct binding at the cell surface and transfer an inhibitory signal to regulate PIN internalization rates (kh_{ij} and kh_{ji}) that is linked with their temporal immobilization at a given side of the cells ($D_C \sim 0$). The green bars represent auxin concentrations in the discrete cell wall compartments.

AUX/LAX family of auxin influx carriers into the cell (Swarup *et al*, 2005; Figure 1A). To exit the cell, auxin required an active transport mediated by the PIN auxin efflux carriers (Petrášek *et al*, 2006; Figure 1A). The auxin diffusion between discrete wall compartments was also taken into account, because of its importance for auxin transport (Swarup *et al*, 2005; Kramer

et al, 2007). Moreover, we considered that the diffusion of auxin was significantly reduced in the apoplast (Kramer *et al*, 2007). On the single-cell level, the ERP model incorporated an auxin-dependent carrier expression (Peer *et al*, 2004; Heisler *et al*, 2005; Vieten *et al*, 2005) that is mediated intracellularly (Figure 1B) by the nuclear TIR1-dependent pathway (Kepinski and Leyser, 2005; Dharmasiri *et al*, 2005). In the model, auxin carriers undergo constitutive degradation in lytic vacuoles (Abas *et al*, 2006; Kleine-Vehn *et al*, 2008b; Figure 1B). The auxin influx carriers (AUX/LAX) were assumed to be uniformly distributed at the plasma membranes, and their targeting mechanisms are considered to be distinct from the PIN proteins (Kleine-Vehn *et al*, 2006; Figure 1C). The dynamics of PIN recycling allowed the translocation of proteins between different cell sides and rapid changes in PIN polarity, as well as in response to various external and internal signals (Benková *et al*, 2003; Friml *et al*, 2002, 2003; Heisler *et al*, 2005; Dhonukshe *et al*, 2008; Kleine-Vehn *et al*, 2008a). Similarly to most recent models (Ibañes *et al*, 2009; Sahlin *et al*, 2009), we included this dynamics of PIN recycling and assumed the auxin-dependent regulation of PIN internalization (Paciorek *et al*, 2005; Figure 1C).

(II) In our model, the concentration-dependent effect of auxin on PIN internalization (Paciorek *et al*, 2005) involved the extracellular receptor-based signaling pathway at the cell surface (Figure 1D), the extracellular pools of hypothetical auxin receptors were shared by each pair of neighboring cells, and the competitive utilization of these auxin receptors allowed direct cell-to-cell communication (Figure 1D). We assumed that auxin binding to the receptor induced signals to inhibit PIN internalization, leading to differential PIN protein retention at different cell sides. Although the direct mode of the signal transfer is unknown, we speculated that bound receptors might be recruited and, hence, temporarily immobilized, to the plasma membrane (or alternatively to cell wall components) for signal transfer, which is modeled by the reduced diffusion of receptors involved in the auxin signaling (Figure 1D). Simultaneously, free receptors from the intercellular pools underwent free diffusion (Figure 1D). To reduce the model complexity, auxin binding to the receptors immediately imposed an inhibitory signal to the nearest cell (Figure 1D). To model the spatial proximity of receptor-based signal transfer to the nearest cell side, we divided the apoplast into two discrete compartments suitable for computational reasons (Figure 1D). The strength of auxin signaling was determined by the amount of auxin-bound receptors present in these discrete wall compartments (Figure 1D).

Analysis of our model revealed that differences in diffusion rates of bound auxin and free receptors are crucial for the model performance. This competitive utilization mechanism enabled cell-to-cell communication in the model, leading to receptor enrichment at the site of increased auxin concentration (Supplementary Figure 1).

We propose that the implementation of these biological data (I) and hypothetical assumptions (II) are sufficient to generate PIN polarity in a given tissue. The model generates initially a weak, diffusion-driven auxin gradient in the apoplast, with asymmetric PIN retention at neighboring cell sides as a consequence (Figure 2A). The competitive utilization of the auxin signaling components would lead to a coordinated asymmetry in PIN internalization rate in the neighboring cells and finally to the alignment of PIN polarity.

Indeed, the synergy of the local auxin signaling between each pair of competing cells promoted tissue polarization (Figure 2B). Intriguingly, this feedback regulation of polar auxin transport contributed to formation of steeper extracellular auxin gradient (Figure 2A and B). In conclusion, the PIN polarization and polar auxin transport both depended on and contributed to the establishment of a differential auxin signaling (Figure 2C and D). Such feedback loop led ultimately to the alignment of PIN polarization within a tissue (Figure 2B).

The ERP model robustly reproduces PIN1 polarity during vascular development

To test whether the ERP model could reproduce the PIN1 polarity patterns observed *in vivo* during vein formation, we used a tissue grid layout and applied minimal assumptions, such as the presence of an auxin source and a distal sink (Figure 3). After auxin application, the simulation revealed that PIN1 polarized away from an auxin source, confirming our theoretical expectations (see above). PIN1 expression was initially broad (Figure 3A and C), but converged over time to a single cell file with strong PIN1 expression and polarization (Figure 3B). This simulation recapitulated the experimental observations during vein formation that PIN1 expression was initially broad with poorly defined polarity (Figure 3E). The addition of an auxin sink was not essential to polarize the PIN proteins (data not shown), but imposed directionality on the developing vein that ultimately linked the auxin source and sink by a PIN-dependent conductive auxin channel.

To analyze behavior, sensitivity, and robustness of the ERP model, we tested the contribution of model components for predicted PIN polarity and auxin distribution patterns. These components include extracellular receptor-based auxin perception and competitive utilization of receptors by neighboring cells (Supplementary Figures 1–3), auxin-mediated carrier expression (Supplementary Figures 4 and 5), PIN- and AUX/LAX-dependent polar transport (Supplementary Figures 6 and 7), and auxin diffusion (Supplementary Figures 8 and 9).

Our model predictions were robust with respect to altered source or sink locations (Supplementary Figure 10) or intracellular auxin gradients (Supplementary Figure 11). The ERP model provided a robust mechanism for canalization of auxin flow (Supplementary Figure 10). Additionally, this model is able to capture conflicting PIN behaviors including PIN polarization with or against the auxin gradient (Supplementary Figures 12–16). During midvein formation, neighboring cells at the advancing edge of the forming vein display transient PIN polarization toward each other (Bayer *et al*, 2009). Intriguingly, the ERP model reproduced this PIN polarization pattern: cells at the growing edge of the forming conductive channel polarized the PIN proteins toward the auxin channel (Figure 3C). In the simulations, the initially weak apoplastic auxin gradient between these cells led to relatively high auxin-dependent inhibition of the PIN endocytosis at the plasma membrane of both cells and, consequently, PIN proteins in neighboring cells became polarized toward

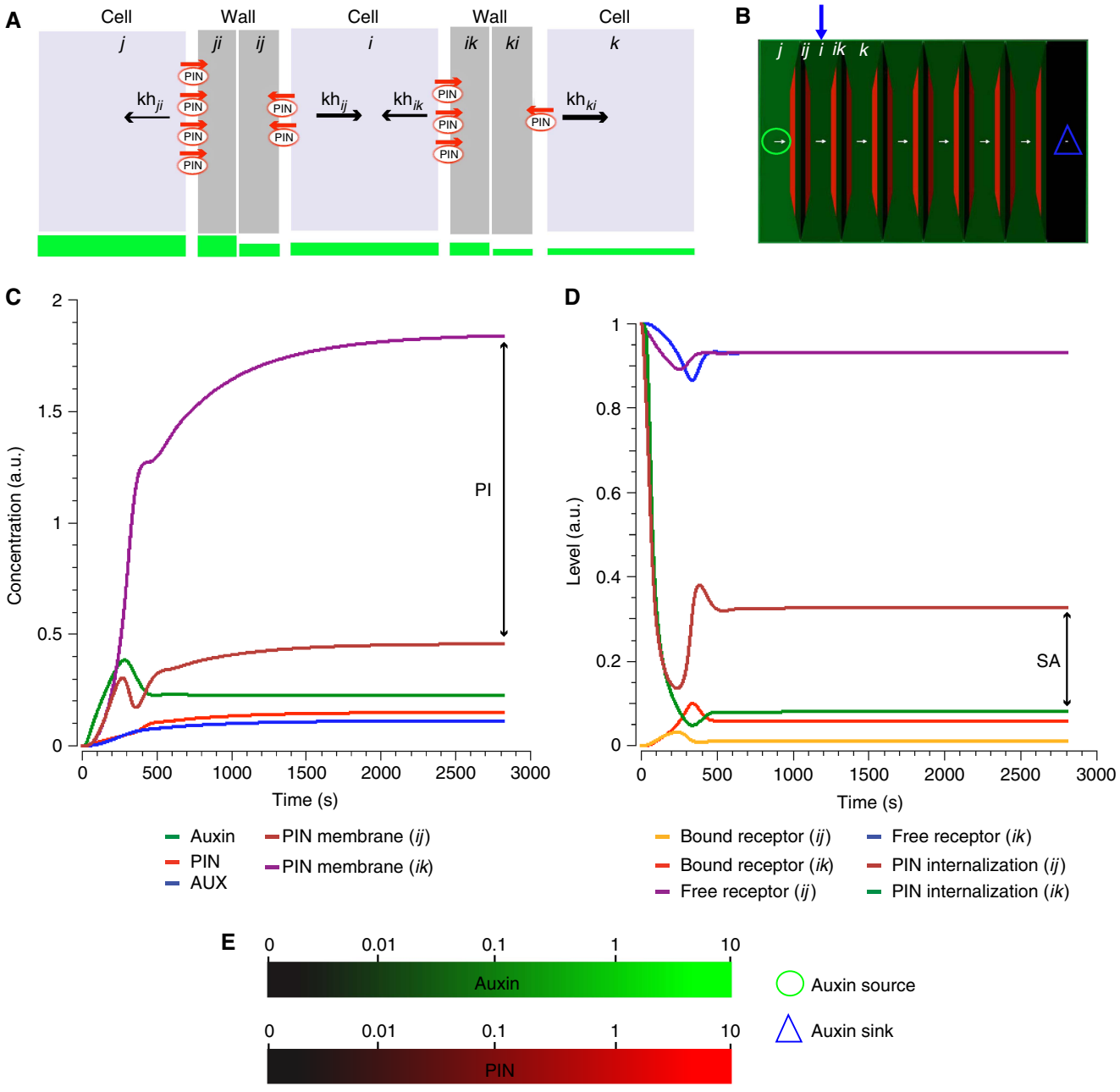

Figure 2 Global polar signal in the cell file produced by the synergy of the local extracellular auxin signaling. (**A**) Schematic representation of a cell file separated by discrete cell wall compartments. Indexes *i*, *j*, and *k* correspond to the three depicted cells. The wall compartments between adjacent pairs of cells are represented by indexes *ji*/*ij* (between cells *i* and *j*) and *ik*/*ki* (between cells *i* and *k*). The component kh with the corresponding index determines the effective rate of the PIN internalization at the given cell side, as described in Figure 1D. PIN (red) abundance at the plasma membrane presumably correlates with the profile of the auxin gradient (green bars). (**B**) *In silico* model simulation on the cell file predicting PIN polarization and canalization of auxin flow. Red and green depict PIN proteins and auxin distribution, respectively. The blue arrow marks the position of the monitored cell in the cell file. (**C**) Time-course profiles of auxin concentration, intracellular PIN and AUX/LAX levels (PIN_i and AUX_i), and PIN membrane levels (PIN_{ij} and PIN_{ik}). (**D**) Time-course profiles of bound (C_{ij} and C_{ik}) and free receptor (R_{ij} and R_{ik}). The levels are normalized by total amount of receptors in the pool (R_T); kh_{ij} and kh_{ik} are the corresponding PIN internalization rates. The polarization index (PI) indicates asymmetry and represents the ratio between PIN levels at the *ik*th plasma membrane and those of the *ij*th membrane (C). The signaling asymmetry (SA) depicts difference in extracellular auxin signaling between *ik*th and *ij*th sides of the cell *i* (D). PI and SA are associated with different states of the cell polarization: no polarization (PI ~ 0, SA ~ 0), initiation of polarization (PI and SA increased), and maintenance of polarization (PI and SA saturated). (**E**) Color coding schemes for auxin concentrations and PIN levels used in all model simulations. Auxin concentrations can vary from 0 (black) to 10 (bright green). PIN levels at the plasma membrane may change from 0 (black) to 10 (bright red). White arrows point in the direction of preferential PIN polarity and the arrow size indicates the relative strength of the PIN expression in the cell. Green circle (source) and blue triangle (sink) illustrate the positions of auxin source and auxin sink on the tissue template.

each other. However, because differences in the auxin transport rates of these neighboring cells (derived from auxin-dependent regulation of auxin carrier expression and polarity) progressively enhanced the extracellular auxin gradient, an enhanced asymmetry in the local auxin signaling was created. The competitive utilization of auxin receptors in

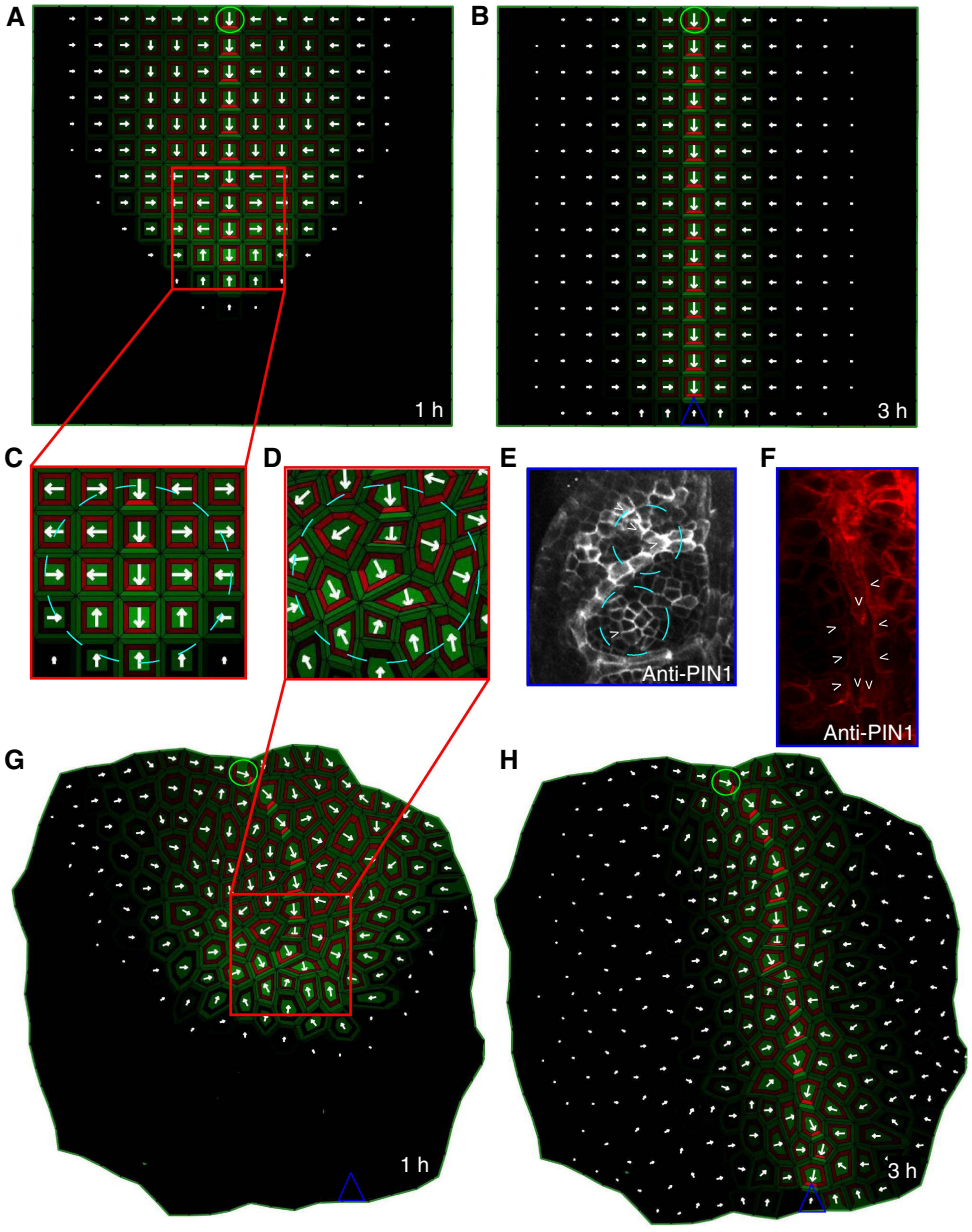

Figure 3 Experimental and simulated PIN-dependent auxin canalization. (**A**–**C**) Simulations of the ERP model on a grid tissue layout. Initially, a broad PIN1 expression domain was predicted (A, C), originating from the site of auxin application (green circle). Subsequently, this expression domain became narrowed to a single cell file, and, finally, produced a conductive auxin channel that connected the auxin source to the distal auxin sink (blue triangle) (B). (**D**, **E**) The broad PIN1 expression domain predicted by the model simulation using the cellular layout (D) and reported *in vivo* in *Arabidopsis* during leaf venation patterning with PIN1 immunolocalization (E). (**F**) PIN polarization during primary vein initiation in young leaves as reported by the PIN1 antibody. Provascular cells show basal PIN1 polarization while the surrounding cells are polarized toward them. (**G**, **H**) ERP model simulation using the cellular tissue layout. The initial, broad PIN1 expression domain (G) becomes reduced to a narrow domain of strong PIN expression (H). The cells adjacent to the vascular strand are polarized toward it (H), as observed *in planta* (F). In the simulations, the PIN proteins are indicated in red and the auxin distribution in green. Green circle (source) and blue triangle (sink) illustrate the positions of auxin source and auxin sink on the tissue template. Arrowheads in panels E and F highlight preferential PIN1 polarization.

the apoplast was necessary for the propagation of differential extracellular auxin signaling and the coordination of PIN polarity within the tissue (Supplementary Figures 1–3). Interestingly, the complete removal of auxin-induced carrier expression from the ERP model did not cause the loss of PIN polarity and auxin canalization in the model simulations (although polarization patterns were less realistic), but only when either the high amount of carriers in the initial pool (Supplementary Figures 4A–L) or high auxin-independent carrier expression (Supplementary Figures 5A–L) were integrated in the model. Next, we tested the ERP model on a more natural tissue layout in which cell shape varied (Figure 3D and G). The model accurately predicted the PIN1 polarization in the natural tissue layout (Figure 3H), recapitulating primary vein formation as observed in leaves (Figure 3F).

For both virtual tissues, the model reproduced the basal PIN1 polarization in provascular cells and lateral PIN1 polarization, pointing toward the conductive auxin channel, in adjacent cells (Figure 3B and G). Interestingly, this observation of lateral PIN1 polarization was absent from the predictions of flux-based models (Mitchison, 1980; Feugier *et al*, 2005; Rolland-Lagan and Prusinkiewicz, 2005). In our model, owing to the high auxin concentrations, the auxin carrier expression is stronger in the conductive channel compared with the adjacent tissues. Furthermore, the PIN-driven efflux is strongly oriented toward the basal cell side of provascular cells while auxin influx remains uniform. This leads to stronger auxin influx compared with auxin efflux at the lateral side of the provascular cell, ultimately triggering the carrier-driven formation of a weak horizontal auxin gradient. In response to this gradient, PIN1 in the neighboring tissues polarized toward the conductive channel. Surprisingly, we found that the activity of the AUX/LAX proteins buffered the motility of auxin in the wall and largely contributed to the maintenance of PIN polarization and auxin gradients in the tissues (Supplementary Figure 7). This finding is consistent with a role of AUX/LAX proteins in phyllotactic patterning (Bainbridge *et al*, 2008).

The ERP simulations suggest the appearance of high auxin concentration in veins

Simulations with the ERP model on tissue layouts predicted PIN1 polarization during the formation of the conductive auxin channel (vein precursor). Other single mechanism-based models, such as flux-based (Mitchison, 1980; Rolland-Lagan and Prusinkiewicz, 2005) and concentration-based models (Merks *et al*, 2007), anticipate low auxin concentrations in the developing veins, which is in contradiction with experimental observations (Scarpella *et al*, 2006). However, several solutions for this problem have been suggested, such as enhanced AUX/LAX-dependent auxin uptake (Kramer, 2004; Swarup *et al*, 2005) or constant total carrier protein abundance (Feugier *et al*, 2005). On the other hand, the ERP model reproduces auxin canalization patterns, involving the dynamic changes in auxin-dependent carrier expression. The auxin concentrations in our model simulations were higher in the emerging veins than in those of surrounding tissues (Figure 4A). An elevation of auxin concentration was observed in provascular cells, whereas neighboring cells showed a steep decrease in auxin concentrations (Figure 4B). This observation might be conceptualized as the balance between PIN1-dependent auxin export from adjacent cells toward the vein precursors and the active drainage of auxin from lateral tissues by AUX/LAX-dependent influx into the provascular cells.

The *in silico* predictions of our model illustrate that high auxin concentrations and high auxin fluxes can simultaneously guide venation patterning, as suggested experimentally (Scarpella *et al*, 2006). Importantly, the ERP model predicted PIN1 polarization not only away from the auxin source but also toward provascular cells with high auxin levels; thus, through a single mechanism, the model recapitulates cell polarization events both away from and toward an auxin maximum.

The ERP model is robust with respect to tissue growth

We successfully utilized the ERP model to reproduce PIN1 polarity in a tissue grid and a more natural tissue layout. To investigate the flexibility and robustness of the model, we additionally imposed a dynamic growth simulation onto the natural tissue layout by assuming that the tissue consecutively expanded and subdivided as the cells changed their size and gave rise to daughter cells (Figure 4C). For more details on modeling growth, we refer to Supplementary information. The growth simulations of the ERP model revealed that (following auxin source and sink application) discrete PIN-dependent auxin channels were maintained within growing cells (cell expansion) and, moreover, were unaffected due to cell division in surrounding tissues (Figure 4D and E). Under these assumptions, the dynamic interplay of intracellular and extracellular auxin signaling might explain the robust adaptation of vascular patterning to tissue growth.

The ERP model reproduces vein connections

The ERP model simulations faithfully reproduced vein formation and progression. Beside single-vein formations, plants have evolved a complex network of connected vasculature. Classical experiments had revealed that preexisting vasculature attracts *de novo* established veins, allowing vein connections to be made (Sachs, 1981), but the underlying mechanism of these inspiring observations remained to be solved.

To study whether the ERP model could provide a theoretical framework to assess the mechanisms underlying these classical experiments, the ERP model was simulated on grid tissue layout and, initially, a single-vein pattern was induced by introducing an auxin source and a distal sink. Next, secondary auxin sources were introduced adjacent to the primary vein (Figure 5A). The simulation showed that a new conductive auxin channel was formed, which originated from the lateral auxin source and ultimately connected to the preexisting vein (Figure 5B). Both *in planta* and *in silico*, it was observed that PIN proteins in the cells that surrounded a conductive auxin channel were polarized toward that channel (Figure 3). In our simulations, it is this preferential lateral polarization toward the auxin-containing channels that leads to the attraction of secondary veins.

The ERP model recapitulates vein loop patterns

Although complex vein networks in leaves are not fully understood, PIN-dependent auxin transport at the leaf margin and auxin biosynthesis appear to initiate vein loop formation (Scarpella *et al*, 2006). To test whether these complex vascular patterns could emerge by using the ERP model, the cellular tissue layout was simulated with an auxin-induced single-vein pattern (Figure 5C–H). As a bipolar PIN1 localization at the side of the vein loop initiation had been observed experimentally (Scarpella *et al*, 2006), we tested whether a bipolar PIN1 signal would be triggered by the sequential introduction of lateral auxin sources in pairs of neighboring cells within the tissue surrounding the main vasculature. Within these pairs of cells, a bipolar PIN1 localization occurred that led to an auxin flow in two

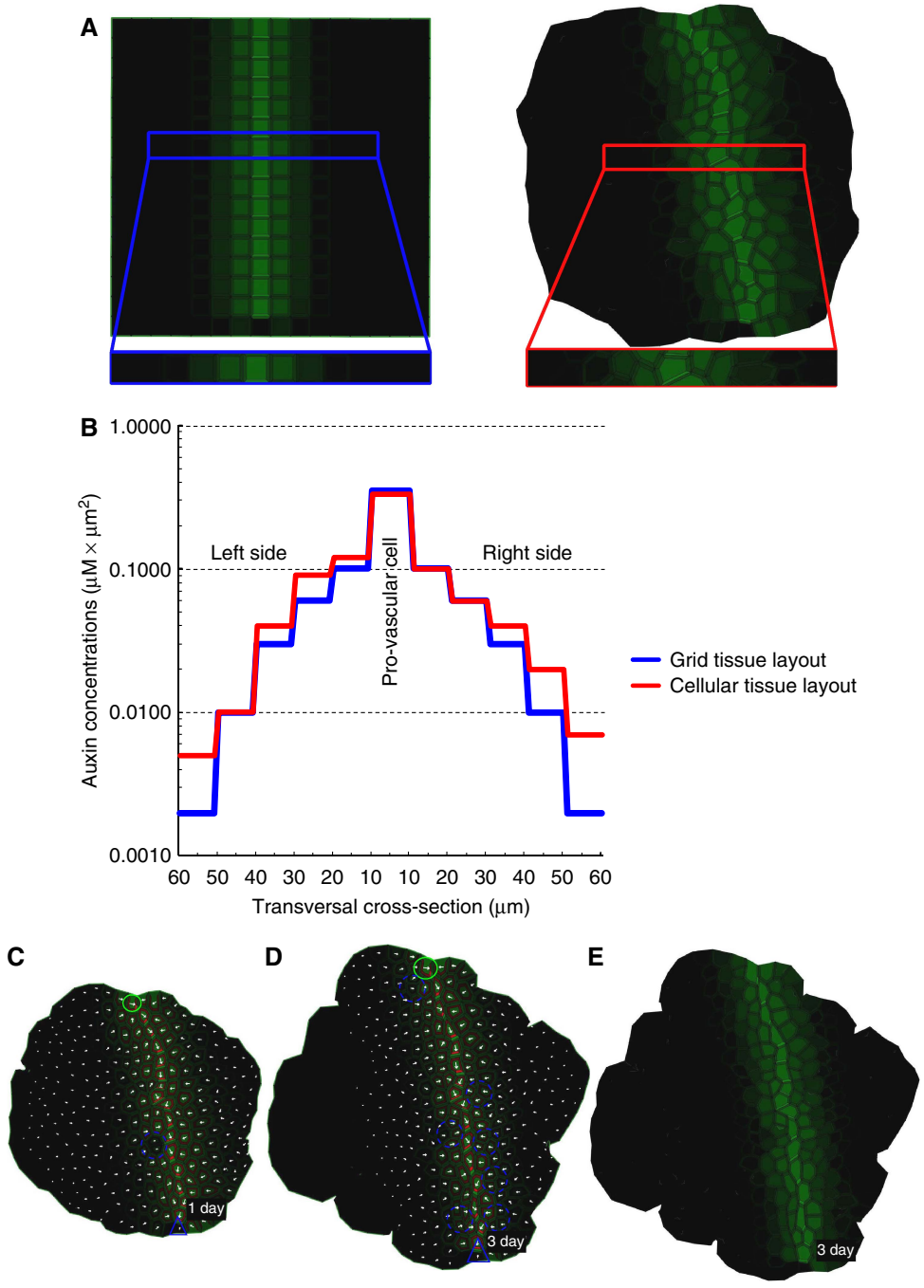

Figure 4 Steady-state auxin distribution patterns during vein propagation and robustness of vein pattern toward tissue growth. (**A**) Steady-state auxin distribution patterns for grid and cellular tissue layouts. (**B**) Examination of the auxin concentrations in cross sections of the tissue layouts showing that the auxin concentration is 10-fold higher in the provascular cells than in the surrounding tissues. (**C**, **D**) Simulation of auxin canalization during dynamic tissue growth. The vein pattern is not altered due to tissue growth. The model predicts PIN1 polarity pattern (C) as observed *in vivo* in *Arabidopsis* (Figure 3E and F). The auxin distribution pattern during tissue growth (**E**) corresponds to that in the non-growing tissue (A). Green circle (source) and blue triangle (sink) illustrate the positions of auxin source and auxin sink on the tissue template. Blue dashed circles highlight the exemplary regions of cell division.

directions from the auxin sources, leaving a trace of polarized cells. Over time, the emerging veins were attracted by the main vein and, finally, formed closed vascular strands (vein loop precursors; Figure 5C–F). The leaf vein loop precursors produced by the simulation contained high auxin concentrations (Figure 5H) and displayed a narrow PIN1 expression domain (Figure 5C–F). These predicted patterns were consistent with the PIN and auxin distribution patterns observed in developing leaves (Figure 5G and H). Additionally, we found that the distance of the lateral auxin sources from the main vasculature might determine the shape, radius, and length of the secondary vein (data not shown).

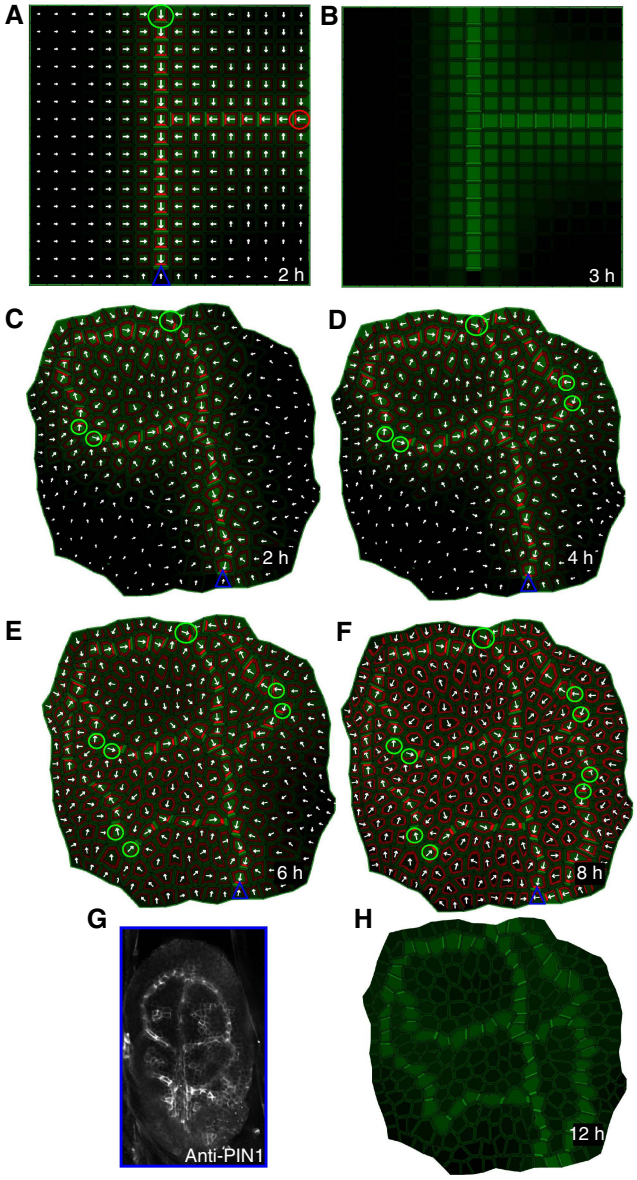

Figure 5 Experimental and simulated auxin distributions and PIN polarization patterns during vein attraction and vein loop formation. (**A**, **B**) *In silico* experiment with the induction of a strong lateral auxin source (red). The main vein attracts the secondary vein, leading to a vascular connection (A). (B) Corresponding steady-state auxin distribution pattern. (**C–F**) Simulation of sequential application of lateral auxin sources (C–F). Sequential addition of lateral auxin sources resulting in a complex vein loop pattern (D), with a predicted PIN1 distribution pattern that is similar to that detected by PIN1 immunolocalization in *Arabidopsis* leaves (**G**). (**H**) Corresponding steady-state auxin concentration pattern revealing high auxin concentration accumulation in vein loops, as observed *in planta* (Scarpella *et al*, 2006). Green circle (source) and blue triangle (sink) illustrate the positions of auxin source and auxin sink on the tissue template.

The ERP model predicts competitive canalization during shoot branching

The ERP model simulations predict that vein connections occur when the lateral auxin source is either comparable with or stronger than the primary auxin source (data not shown). This finding suggests that the interconnection of vascular systems might depend on the actual auxin concentration ratio between competing auxin sources, a relation reminiscent to a process proposed to regulate shoot branching. Auxin production and auxin flow in the primary shoot impose an apical dominance over lateral buds and inhibit their outgrowth (Thimann and Skoog, 1933). The removal of the apical auxin source, for instance by decapitation, leads to bud outgrowth. A competitive auxin transport mechanism between the dormant bud and stem vasculature has been proposed to regulate bud outgrowth (Prusinkiewicz *et al*, 2009; Balla *et al*, 2010). Accordingly, dormant buds fail to polarize PIN proteins and establish a PIN-dependent auxin flow and vein connection to the main vein in the stem, limiting their developmental progression.

To investigate whether the temporal supremacy of the primary auxin source in the system might be the actual reason for the inhibition of vein connection, we simulated the ERP model on grid tissue layout (stem representation), with a dominant apical auxin source and a distal auxin sink to induce a primary vein. Subsequently, we reduced the strength of the primary auxin source, which could correspond to virtual stem decapitation (Figure 6A). Afterward, we introduced a secondary lateral auxin source (Figure 6B). Over time, vein connection was observed from the lateral auxin source, following PIN1 polarization toward the primary vein (Figure 6C–E). To verify the model outcome experimentally, we studied the PIN1 localization by immunolocalization with a PIN1 antibody in pea (*Pisum sativum*) stems. After stem decapitation (Figure 6F), exogenous application of auxin to the lateral site of the stem resulted in PIN1 expression at the site of application and polarization of PIN1 toward the preexisting vasculature (Figure 6G and H). To substantiate this finding, we reactivated the primary auxin source after stem decapitation (Figure 6I and J), before the virtual application of the secondary auxin source (Figure 6K). Under this condition, the lateral auxin source failed to connect to the primary vasculature (Figure 6L and M), which could be validated by performing PIN1 immunolocalizations on pea stems to which an apical auxin source had been applied after decapitation (Figure 6N–P).

The observations from the model simulations and experiments imply that the temporal supremacy of primary over secondary auxin sources is presumably determined by the relative strength of the sources. To support this conclusion, we analyzed the behavior of the ERP model under the variable strength of auxin input in the system (Supplementary Figure 12). The dynamic instabilities characterized by periodic oscillations of PIN polarization in the presence of a weak auxin source corresponded to the absence of vein connection (vein repulsion) (Supplementary Figures 12M–P). In contrast, an increase of the overall auxin concentrations in the tissue caused by the presence of an enhanced auxin source led to the stable formation of vein patterns (Supplementary Figures 12E–L). These findings are in agreement with experimental and theoretical observations based on PIN-dependent auxin transport (Prusinkiewicz *et al*, 2009).

The ERP simulations revealed simple, yet important, mechanistic insights into this type of competitive inhibition

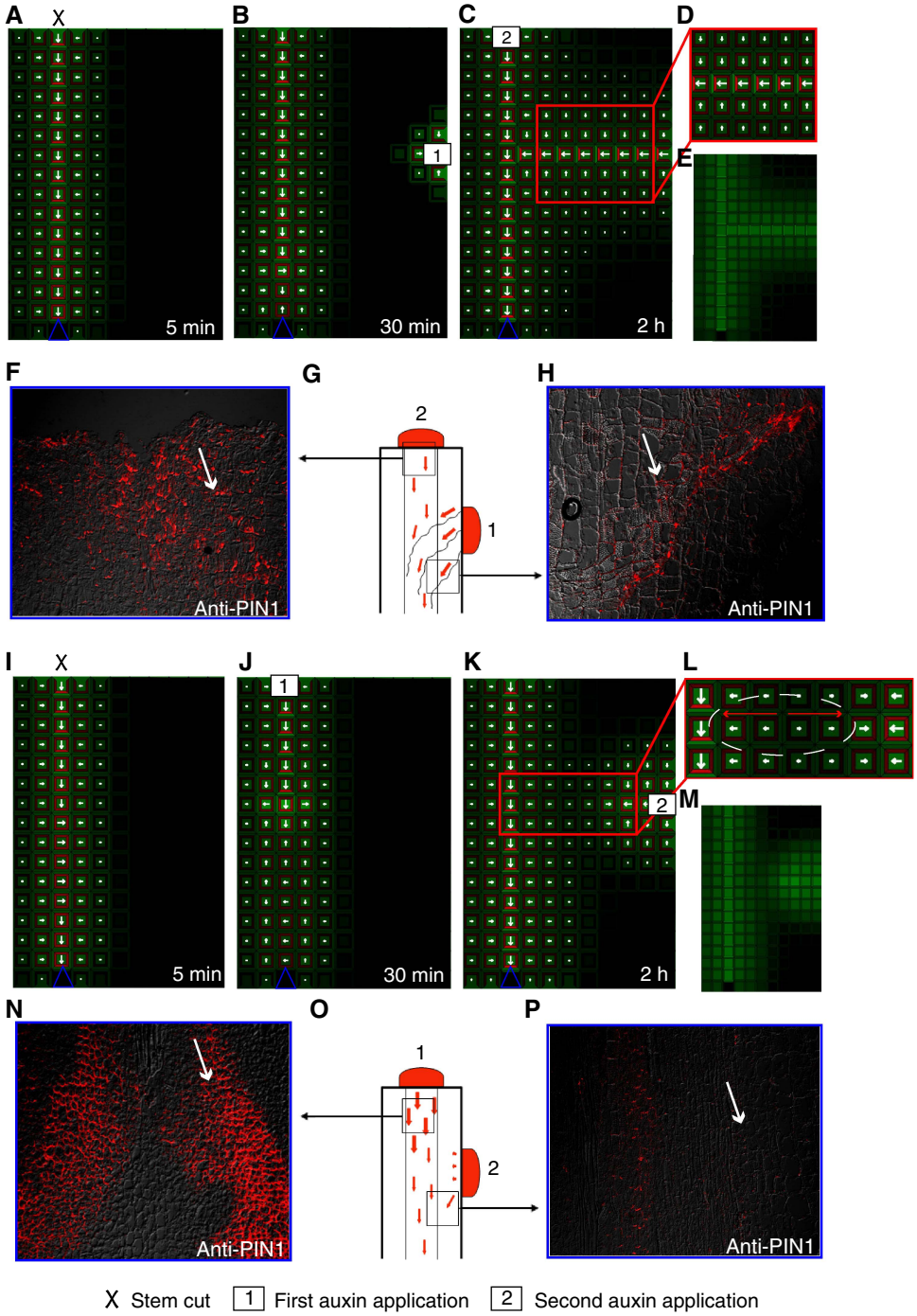

Figure 6 Experimental and simulated auxin distributions and PIN polarization patterns during branching activation and inhibition. (**A**–**E**) Simulation of a virtual stem cut (A) and subsequent virtual auxin applications, first to the lateral site (B) and second to the apical site (C). (D) Unilateral PIN1 polarity in the proximity of the main vein and canalization from the lateral auxin source, as predicted by ERP model (E). (**F**–**H**) PIN1 immunolocalization in pea stems after decapitation (F, H) (Balla *et al*, 2010). Auxin was applied first laterally and then apically (G). Canalization from the lateral source occurs analogously to that from a secondary auxin source (F, H). (**I**–**M**) Simulations of a virtual stem cut (I) and subsequent virtual auxin application, first to the apical site (J) and second to the lateral side of the tissue (K). (L) Bipolar PIN1 polarity in the cells between the main vein and the lateral source, resulting in the lack of vein connection (M). (**N**–**P**) PIN1 immunolocalization in pea stems after decapitation and subsequent auxin application (N, P) (Balla *et al*, 2010). Auxin was applied first to the apical site and then to the lateral site (O). Canalization from the lateral source did not occur (P). Blue triangle (sink) illustrate the positions of auxin sink on the tissue template. Arrows in panels F, H, N and P highlight preferential PIN1 polarization.

that had initially been proposed to explain branching patterns in plants (Prusinkiewicz *et al*, 2009). Our simulations faithfully reproduced PIN polarization toward the existing conductive auxin channel and preferential PIN polarization toward the newly forming auxin channel. However, the pattern of PIN polarization at the growing tip of the channel led to

adverse PIN polarization in the proximity of the main vein (Figure 6L). Accordingly, the auxin concentration in the emerging lateral vein precursor needed to be comparable with or higher than that in the main vein to break this adverse polarization and to establish a vein connection (Figure 6C and Supplementary Figure 12). Thus, our modeling and experimental results provide a strong support for the hypothesis of competitive auxin canalization (Prusinkiewicz *et al*, 2009) proposed for shoot branching in plants.

Self-organization and dynamics of the ERP model explain PIN polarity rearrangements during vascular regeneration

The ERP model accounted for vascular patterning processes, such as vein formation and propagation, competitive vein attraction/repulsion, and vein loop formation. Next, we studied another interesting aspect of vascular patterning linked to the regeneration of plant vasculature after local tissue wounding. Local wounding during tissue regeneration stimulates rearrangements in the polar localization of PIN proteins, thus providing plants with a flexible developmental adaptation (Benková *et al*, 2003; Sauer *et al*, 2006). We tested the ERP model for changes in PIN polarity and auxin distribution associated with the regeneration of vasculature after wounding. First, we simulated an apical auxin source and distal auxin sink to establish an initial steady-state vein pattern. Subsequently, we disrupted this pattern by introducing virtual wounding (cell ablation; Figure 7A–C). A few minutes after wounding, auxin accumulated above the wound (Figure 7D), after which the PIN1 proteins were re-polarized. These flexible polarity rearrangements led to the regeneration of a conductive auxin channel circumventing the ablated cells (Figure 7E; Sauer *et al*, 2006). Additionally, the model simulation suggested a transient downregulation of the *PIN1* expression below the ablated cells (Figure 7F) that had not been reported previously.

To test these observations experimentally, we used a PIN1 antibody to study PIN1 distribution after wounding in pea stems. Tissue ablation resulted in a reduction in PIN1 expression just below the wound (Figure 7G). The PIN polarity pattern observed after *de novo* vascular regeneration (Figure 7G) was very similar to that predicted by the ERP model (Figure 7H and I).

The whole sequence of events predicted by the model, including auxin accumulation above the wound and PIN polarization around the wound, are consistent with previous experimental findings (Sauer *et al*, 2006). The model forecasts that the ectopic accumulation of auxin (new sources) above the wound and the decrease in auxin content below the wound (new sinks) is the actual trigger for vein regeneration. Accordingly, high auxin above the wound functions as a new auxin source that leads to PIN polarization toward the tissues with low auxin concentration below the wound. Concomitantly, the auxin-induced carrier expression integrated in the ERP model was necessary to facilitate this PIN re-polarization during vein regeneration (Supplementary Figures 4M–P and 5M–P), suggesting a temporal downregulation of PIN expression in the surroundings of the ablated region, ectopic auxin accumulation above the wound, and *de novo* PIN synthesis facilitating rearrangement of PIN polarity and guiding the regeneration of tissues.

Discussion

A unique feature of auxin among the plant hormones is its tightly regulated, cell-to-cell polar transport that allows auxin to convey positional and directional signals between cells and to contribute to tissue polarization and patterning. Here, we validate a conceptually novel mechanism for polarization of auxin transport in plant tissues. Our computer model integrates up-to-date cell biological data and a minimal theoretical framework for an auto-regulatory positive feedback loop between auxin and its polar redistribution of PIN auxin transporters. The subcellular dynamics of auxin carriers and auxin feedback on carrier expression that have been reported experimentally are both integrated into our model. Additionally, the model provides a mechanistically plausible framework for extracellular receptor-based auxin regulation for spatiotemporal synchronization and coordination of cell polarity, which, to our knowledge, had never been exploited in previous theoretical or experimental studies.

We propose that plant cells compete for extracellular auxin receptors to establish their polarities within tissues. Neither the auxin gradients in the cell wall nor the competitive utilization of receptors in the extracellular space had been so-far considered for spatial-temporal regulation of the PIN abundance at the plasma membrane (Sahlin *et al*, 2009).

We demonstrated the plausibility of the ERP model for various processes, including *de novo* vascularization, venation patterning, and tissue regeneration in computer simulations performed with only minimal initial assumptions, namely a discrete auxin source and a distal sink. Moreover, these simulations were robust with respect to variable conditions, such as tissue growth, membrane permeability, auxin diffusion and auxin carrier expression levels, and position of auxin sources/sinks.

The ERP model reproduces the very detailed PIN polarization events that occur during primary vein initiation (Scarpella *et al*, 2006), such as basal PIN polarity in provascular cells, transient adverse PIN polarization in neighboring cells during the alignment of tissue polarization, and inner-lateral polarity displayed by the tissues surrounding a conductive auxin channel. Additionally, the ERP model generates high auxin concentration and high auxin flux simultaneously in emerging veins, revising the classical canalization models (Mitchison, 1980; Rolland-Lagan and Prusinkiewicz, 2005). Importantly, all the simulations support the claim that the ERP model represents the first single approach that faithfully reproduces the PIN polarization, both with the auxin gradient (basal PIN1 polarity in provascular cells) and against the auxin gradient (transient adverse PIN1 polarization in neighboring cells surrounding the provascular bundle), as well as producing the corresponding auxin distribution patterns during auxin canalization.

Interestingly, the ERP model predicts that minimal assumptions, such as the regulated position and strength of auxin sources, are sufficient to explain (i) the source-to-sink guided organization of complex venation patterns (loops) at the base

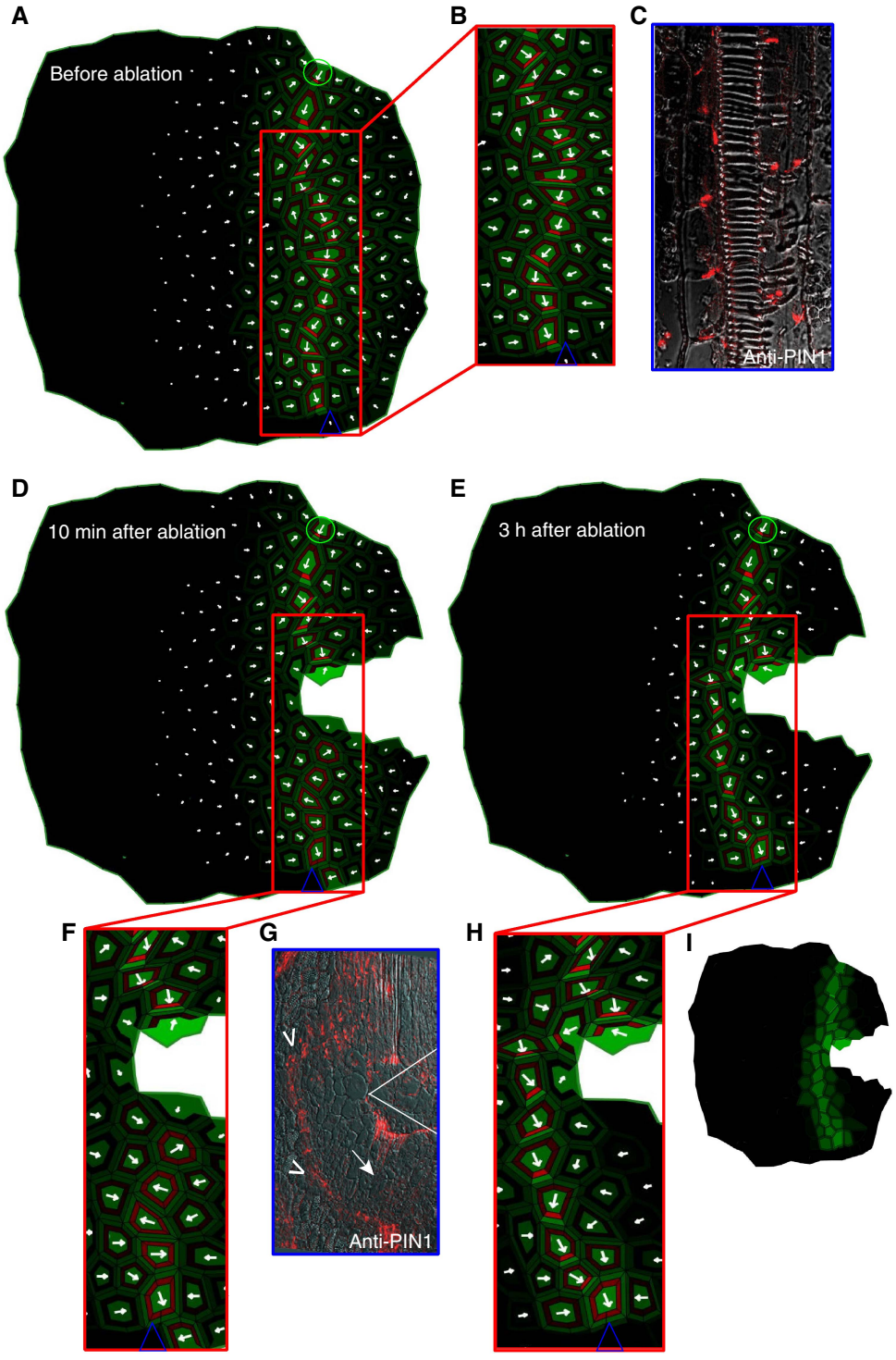

Figure 7 Experimental and simulated rearrangement of PIN polarity after wounding. (**A**–**C**) PIN1 polarization pattern in the model simulation (A and B) and in a *pea* stem (C) before tissue ablation. (**D**) Downregulation of PIN1 expression below the wound apparent immediately after wounding. (**E**) Restoration of the vascular pattern by circumvention of the ablated cells. (**F**–**H**) Enlarged views of the wound site. PIN1 downregulation in response to wounding in the model simulation (F), and in the *pea* wounding experiment (G), as reported with the PIN1 antibody (white arrow). The predicted PIN polarization pattern after vein regeneration (H) is similar to that observed in the pea stem (G) as indicated by the white arrowheads. (**I**) Auxin distribution pattern revealing the auxin accumulation site just above the ablated cells. Green circle (source) and blue triangle (sink) illustrate the positions of auxin source and auxin sink on the tissue template.

of a leaf solely by the read out of localized auxin concentration spots (Scarpella *et al*, 2006) and (ii) the actual magnitude of auxin sources as a self-reliant signal to control mutual auxin source competition for vascular connection, for instance during the auxin transport regulation of shoot branching. The model simulations revealed that the generation of these

complex and often transient PIN polarities is a self-emerging property of the ERP model. Importantly, the stability of these complex polarities is regulated by auxin in a concentration-dependent manner that provides a new explanation for vein attraction and repulsion phenomena.

Finally, we have demonstrated that the self-organizing dynamics of the ERP model produce a system that is able to adapt to external disruptions and provide a mechanistic framework for processes such as vascular tissue regeneration (Sauer *et al*, 2006). By guiding a switch in PIN polarization and creating the associated temporal changes in auxin accumulation, a flexible pattern was created that allows the plant to adapt. The model analysis revealed the necessity of tight regulation of carrier expression by auxin for vascular patterning and regeneration after wounding. The ERP model simulations also illustrate how macroscopically different developmental processes, such as vascular tissue formation and apical dominance-controlled shoot branching, can be unified by a single mechanism derived through the combination of intracellular auxin feedback on carrier expression and extracellular perception-based regulation of the auxin carrier trafficking.

Here, we propose that extracellular auxin signaling facilitated by high-affinity binding of auxin to its extracellular receptor is essential to account for coordinated polarization of PIN proteins and auxin canalization during vascular development. The putative candidate for extracellular auxin receptor is ABP1 that resides in the lumen of the endoplasmic reticulum and is secreted to the cell wall (Napier *et al*, 2002) where it is physiologically active (Leblanc *et al*, 1999; Steffens *et al*, 2001). Auxin inhibits clathrin-dependent PIN internalization via binding to ABP1 (Robert *et al*, 2010). However, ABP1 and its contribution to coordinated tissue polarity still needs to be experimentally investigated (Tromas *et al*, 2009). Such extracellular fraction of ABP1 (or yet to be identified ABPs) could correspond to the intercellular pools of extracellular auxin receptors in the ERP model. It still remains to be tested whether the ERP model could account for complex PIN polarity and auxin distribution patterns associated with embryogenesis, root system maintenance, and *de novo* organ formation.

Materials and methods

Computational methods

For model description, parameters, sensitivity analysis, and simulation insets, we refer to Supplementary information. The model was based on a version of *VirtualLeaf* (Merks *et al*, 2007; Merks *et al*, 2010), a cell-based simulation tool for modeling plant development. All simulations were run until steady-state patterns emerged. All figures were processed in Adobe Illustrator. Figures 3–7 and Supplementary movies 1-7 are screenshots from the model simulations. The VirtualLeaf binaries with the ERP model definitions (pseudo C++ source) are available on the public website http://users.UGent.be/~kwabnik.

Experimental methods

Whole-mount immunolocalizations in *Arabidopsis thaliana* (L.) *Heyhn* leaves were carried out as described (Friml *et al*, 2003) and in pea (*Pisum sativum*) on 5-mm longitudinal epicotyl sections according to the method established and described for *Arabidopsis* stems (Friml *et al*, 2003). The anti-*Arabidopsis* PIN1 antibody also recognized a polarly localized homologous PIN protein in pea (Sauer *et al*, 2006). The following antibodies and dilutions were used: anti-PIN1 (1:500), FITC- and CY3-conjugated anti-rabbit (1:500), or anti-mouse (1:500). For wounding experiments, pea seedlings were used 5 days after germination. Incisions to 70–80% of the stem diameter were made on epicotyls between the cotyledons and the first axillary bud. Wounded tissue was separated with plastic film. At least 20 epicotyls from two independent experiments were analyzed. After the treatments, epicotyl sections were fixed, embedded in paraffin, and processed for anti-PIN1 immunocytochemistry as described (Friml *et al*, 2003).

Specimens were viewed under a confocal laser-scanning microscope TCS SP2 AOBS (Leica; http://www.leica-microsystems.com) with a $\times$10/0.4, $\times$20/0.7, or $\times$63/1.4 objective at room temperature or with Fluoview 200 (Olympus; http://www.olympusfluoview.com) and a $\times$20/0.50 objective at room temperature. Images were acquired with the Leica confocal software 2.00 or Fluoview 5.1 software, saved as TIF files, processed with Adobe Photoshop 7.0 (http://www.adobe.com), and adjusted for brightness and contrast.

Supplementary information

Supplementary information is available at the *Molecular Systems Biology* website (www.nature.com/msb).

Acknowledgements

We thank Angharad Jones for critical reading of the paper, Przemyslaw Prusinkiewicz for fruitful discussions and comments, and Martine De Cock for help in preparing it. This work was supported by grants from the Research Foundation-Flanders (Odysseus) and Grant Agency of the Academy of Sciences of the Czech Republic Grant IAA601630703 to JF, the Research Foundation-Flanders (project no. 3G006507) to WG, Marie Curie European Reintegration Grant 230974 to RMHM, and Czech Ministry of Education LC06034 to JB This work was co-financed by the Netherlands Consortium for Systems Biology (NCSB), which is part of the Netherlands Genomics Initiative/Netherlands Organization for Scientific Research. JF, JK-V, KW, RMHM, WG designed the experiments; KW, JK-V, MS, JB, SN performed the experiments; KW, JK-V and JF wrote the paper.

Conflict of interest

The authors declare that they have no conflict of interest.

References

Abas L, Benjamins R, Malenica N, Paciorek T, Wiśniewska J, Moulinier-Anzola JC, Sieberer T, Friml J, Luschnig C (2006) Intracellular trafficking and proteolysis of the *Arabidopsis* auxin-efflux facilitator PIN2 are involved in root gravitropism. *Nat Cell Biol* **8:** 249–256

Bainbridge K, Guyomarc'h S, Bayer E, Swarup R, Bennett M, Mandel T, Kuhlemeier C (2008) Auxin influx carriers stabilize phyllotactic patterning. *Genes Dev* **22:** 810–823

Balla J, Kalousek P, Reinöhl V, Friml J, Procházka S (2010) Competitive canalization of PIN-dependent auxin flow from axillary buds controls pea bud outgrowth. *Plant J* (in press)

Bayer EM, Smith RS, Mandel T, Nakayama N, Sauer M, Prusinkiewicz P, Kuhlemeier C (2009) Integration of transport-based models for phyllotaxis and midvein formation. *Genes Dev* **23:** 373–384

Benková E, Michniewicz M, Sauer M, Teichmann T, Seifertová D, Jürgens G, Friml J (2003) Local, efflux-dependent auxin gradients as a common module for plant organ formation. *Cell* **115:** 591–602

Chapman EJ, Estelle M (2009) Mechanism of auxin-regulated gene expression in plants. *Annu Rev Genet* **43:** 265–285

Darwin C, Darwin F (1880) *The Power of Movement in Plants*. London, John Murray, pp 592

Dharmasiri N, Dharmasiri S, Estelle M (2005) The F-box protein TIR1 is an auxin receptor. *Nature* **435:** 441–445

Dhonukshe P, Aniento F, Hwang I, Robinson DG, Mravec J, Stierhof Y-D, Friml J (2007) Clathrin-mediated constitutive endocytosis of PIN auxin efflux carriers in *Arabidopsis*. *Curr Biol* **17:** 520–527

Dhonukshe P, Tanaka H, Goh T, Ebine K, Mähönen AP, Prasad K, Blilou I, Geldner N, Xu J, Uemura T, Chory J, Ueda T, Nakano A, Scheres B, Friml J (2008) Generation of cell polarity in plants links endocytosis, auxin distribution and cell fate decisions. *Nature* **456:** 962–966

Dubrovsky JG, Sauer M, Napsucialy-Mendivil S, Ivanchenko MG, Friml J, Shishkova S, Celenza J, Benková E (2008) Auxin acts as a local morphogenetic trigger to specify lateral root founder cells. *Proc Natl Acad Sci USA* **105:** 8790–8794

Feugier FG, Mochizuki A, Iwasa Y (2005) Self-organization of the vascular system in plant leaves: inter-dependent dynamics of auxin flux and carrier proteins. *J Theor Biol* **236:** 366–375

Friml J, Vieten A, Sauer M, Weijers D, Schwarz H, Hamann T, Offringa R, Jürgens G (2003) Efflux-dependent auxin gradients establish the apical–basal axis of *Arabidopsis*. *Nature* **426:** 147–153

Friml J, Wiśniewska J, Benková E, Mendgen K, Palme K (2002) Lateral relocation of auxin efflux regulator PIN3 mediates tropism in *Arabidopsis*. *Nature* **415:** 806–809

Geldner N, Friml J, Stierhof Y-D, Jürgens G, Palme K (2001) Auxin transport inhibitors block PIN1 cycling and vesicle trafficking. *Nature* **413:** 425–428

Goldsmith MHM, Goldsmith TH, Martin MH (1981) Mathematical analysis of the chemosmotic polar diffusion of auxin through plant tissues. *Proc Natl Acad Sci USA* **78:** 976–980

Heisler MG, Ohno C, Das P, Sieber P, Reddy GV, Long JA, Meyerowitz EM (2005) Patterns of auxin transport and gene expression during primordium development revealed by live imaging of the *Arabidopsis* inflorescence meristem. *Curr Biol* **15:** 1899–1911

Ibañes M, Fàbregas N, Chory J, Caño-Delgado AI (2009) Brassinosteroid signaling and auxin transport are required to establish the periodic pattern of *Arabidopsis* shoot vascular bundles. *Proc Natl Acad Sci USA* **106:** 13630–13635

Jönsson H, Heisler MG, Shapiro BE, Meyerowitz EM, Mjolsness E (2006) An auxin-driven polarized transport model for phyllotaxis. *Proc Natl Acad Sci USA* **103:** 1633–1638

Kepinski S, Leyser O (2005) The *Arabidopsis* F-box protein TIR1 is an auxin receptor. *Nature* **435:** 446–451

Kleine-Vehn J, Friml J (2008) Polar targeting and endocytic recycling in auxin-dependent plant development. *Annu Rev Cell Dev Biol* **24:** 447–473

Kleine-Vehn J, Dhonukshe P, Sauer M, Brewer P, Wiśniewska J, Paciorek T, Benková E, Friml J (2008a) ARF GEF-dependent transcytosis and polar delivery of PIN auxin carriers in *Arabidopsis*. *Curr Biol* **18:** 526–531

Kleine-Vehn J, Dhonukshe P, Swarup R, Bennett M, Friml J (2006) Subcellular trafficking of the *Arabidopsis* auxin influx carrier AUX1 uses a novel pathway distinct from PIN1. *Plant Cell* **18:** 3171–3181

Kleine-Vehn J, Leitner J, Zwiewka M, Sauer M, Abas L, Luschnig C, Friml J (2008b) Differential degradation of PIN2 auxin efflux carrier by retromer-dependent vacuolar targeting. *Proc Natl Acad Sci USA* **105:** 17812–17817

Kramer EM (2004) PIN and AUX/LAX proteins: their role in auxin accumulation. *Trends Plant Sci* **9:** 578–582

Kramer EM (2009) Auxin-regulated cell polarity: an inside job? *Trends Plant Sci* **14:** 242–247

Kramer EM, Frazer NL, Baskin TI (2007) Measurement of diffusion within the cell wall in living roots of *Arabidopsis thaliana*. *J Exp Bot* **58:** 3005–3015

Leblanc N, David K, Grosclaude J, Pradier J-M, Barbier-Brygoo H, Labiau S, Perrot-Rechenmann C (1999) A novel immunological approach establishes that the auxin-binding protein, Nt-abp1, is an element involved in auxin signaling at the plasma membrane. *J Biol Chem* **274:** 28314–28320

Merks RMH, Guravage M, Inzé D, Beemster GTS (2010) VirtualLeaf: an Open Source framework for cell-based modeling of plant tissue growth and development. *Plant Physiol* (in press)

Merks RMH, Van de Peer Y, Inzé D, Beemster GTS (2007) Canalization without flux sensors: a traveling-wave hypothesis. *Trends Plant Sci* **12:** 384–390

Mitchison GJ (1980) The dynamics of auxin transport. *Proc R Soc Lond B* **209:** 489–511

Napier RM, David KM, Perrot-Rechenmann C (2002) A short history of auxin-binding proteins. *Plant Mol Biol* **49:** 339–348

Paciorek T, Zažímalová E, Ruthardt N, Petrášek J, Stierhof Y-D, Kleine-Vehn J, Morris DA, Emans N, Jürgens G, Geldner N, Friml J (2005) Auxin inhibits endocytosis and promotes its own efflux from cells. *Nature* **435:** 1251–1256

Peer WA, Bandyopadhyay A, Blakeslee JJ, Makam SN, Chen RJ, Masson PH, Murphy AS (2004) Variation in expression and protein localization of the PIN family of auxin efflux facilitator proteins in flavonoid mutants with altered auxin transport in *Arabidopsis thaliana*. *Plant Cell* **16:** 1898–1911

Petrášek J, Mravec J, Bouchard R, Blakeslee JJ, Abas M, Seifertová D, Wiśniewska J, Tadele Z, Kubeš M, Ovanová M, Dhonukshe P, Skůpa P, Benková E, Perry L, Křeček P, Lee OR, Fink GR, Geisler M, Murphy AS, Luschnig C *et al* (2006) PIN proteins perform a rate-limiting function in cellular auxin efflux. *Science* **312:** 914–918

Prusinkiewicz P, Crawford S, Smith RS, Ljung K, Bennett T, Ongaro V, Leyser O (2009) Control of bud activation by an auxin transport switch. *Proc Natl Acad Sci USA* **106:** 17431–17436

Reinhardt D, Pesce E-R, Stieger P, Mandel T, Baltensperger K, Bennett M, Traas J, Friml J, Kuhlemeier C (2003) Regulation of phyllotaxis by polar auxin transport. *Nature* **426:** 255–260

Robert S, Kleine-Vehn J, Barbez E, Sauer M, Paciorek T, Baster P, Vanneste S, Zhang J, Simon S, Hayashi K, Dhonukshe P, Yang Z, Bednarek SY, Jones AM, Aniento F, Zažímolová E, Friml J (2010) ABP1 mediates auxin inhibition of clathrin-dependent endocytosis in Arabidopsis. *Cell* **143:** 111–121

Rolland-Lagan A-G, Prusinkiewicz P (2005) Reviewing models of auxin canalization in the context of leaf vein pattern formation in Arabidopsis. *Plant J* **44:** 854–865

Sachs T (1981) The control of the patterned differentiation of vascular tissues. *Adv Bot Res* **9:** 151–262

Sahlin P, Söderberg B, Jönsson H (2009) Regulated transport as a mechanism for pattern generation: capabilities for phyllotaxis and beyond. *J Theor Biol* **258:** 60–70

Sauer M, Balla J, Luschnig C, Wiśniewska J, Reinöhl V, Friml J, Benková E (2006) Canalization of auxin flow by Aux/IAA-ARF-dependent feed-back regulation of PIN polarity. *Genes Dev* **20:** 2902–2911

Scarpella E, Marcos D, Friml J, Berleth T (2006) Control of leaf vascular patterning by polar auxin transport. *Genes Dev* **20:** 1015–1027

Smith RS, Guyomarc'h S, Mandel T, Reinhardt D, Kuhlemeier C, Prusinkiewicz P (2006) A plausible model of phyllotaxis. *Proc Natl Acad Sci USA* **103:** 1301–1306

Steffens B, Feckler C, Palme K, Christian M, Böttger M, Lüthen H (2001) The auxin signal for protoplast swelling is perceived by extracellular ABP1. *Plant J* **27:** 591–599

Swarup R, Kramer EM, Perry P, Knox K, Leyser HMO, Haseloff J, Beemster GTS, Bhalerao R, Bennett MJ (2005) Root gravitropism requires lateral root cap and epidermal cells for transport and response to a mobile auxin signal. *Nat Cell Biol* **7:** 1057–1065

Thimann KV, Skoog F (1933) Studies on the growth hormone of plants. III. The inhibiting action of the growth substance on bud development. *Proc Natl Acad Sci USA* **19:** 714–716

Tromas A, Braun N, Muller P, Khodus T, Paponov IA, Palme K, Ljung K, Lee J-Y, Benfey P, Murray JAH, Scheres B, Perrot-Rechenmann C

(2009) The AUXIN BINDING PROTEIN 1 is required for differential auxin responses mediating root growth. *PLoS One* **4:** e6648

Vieten A, Vanneste S, Wiśniewska J, Benková E, Benjamins R, Beeckman T, Luschnig C, Friml J (2005) Functional redundancy of PIN proteins is accompanied by auxin-dependent cross-regulation of PIN expression. *Development* **132:** 4521–4531

Wiśniewska J, Xu J, Seifertová D, Brewer PB, Růžička K, Blilou I, Rouquié D, Benková E, Scheres B, Friml J (2006) Polar PIN localization directs auxin flow in plants. *Science* **312:** 883

Real data.
Real installations.
Real super-resolution imaging.

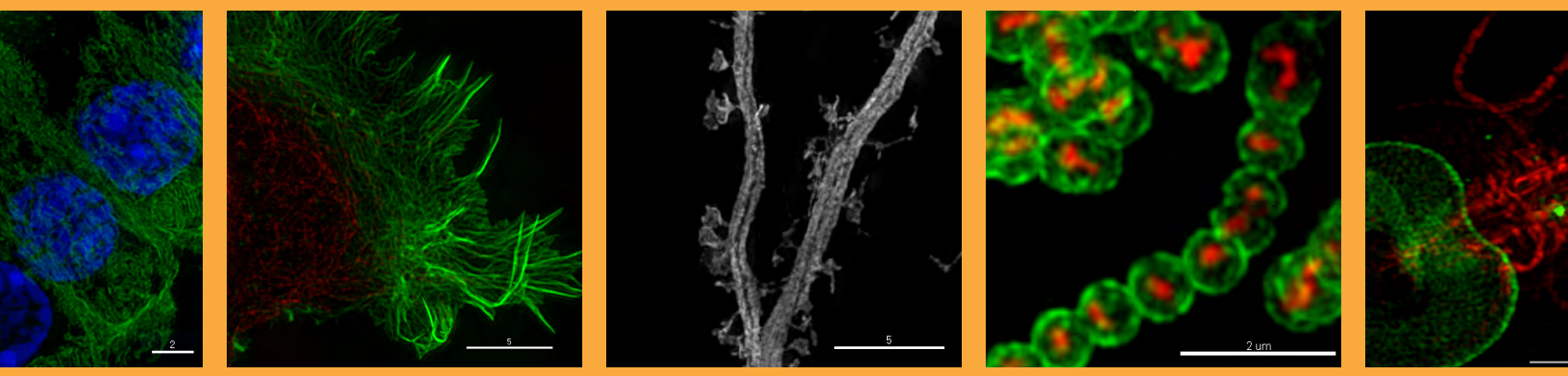

Learn more about the DeltaVision OMX super-resolution imaging system at **www.superresolution.com**.

applied precision

1040 12th Ave NW | Issaquah, WA 98027